VILNIUS UNIVERSITY,

INSTITUTE OF PHYSICS OF

CENTER FOR PHYSICAL SCIENCES AND TECHNOLOGY

Pranciškus Vitta

FREQUENCY-RESOLVED SPECTROSCOPY OF RELAXATION PROCESES IN OPTOELECTRONIC MATERIALS AND DEVICES

Summary of doctoral thesis
Physical Sciences, Physics – 02 P

Vilnius, 2010

The research has been carried out in 2006-2010 at the Semiconductor Physics Department of Physics Faculty and Institute of Applied Research, Vilnius University.

Scientific supervisor:

Prof. habil. dr. Artūras Žukauskas (Vilnius University, Physical Sciences, Physics – 02 P).

Consultant:

Prof. habil. dr. Gintautas Tamulaitis (Vilnius University, Physical Sciences, Physics – 02 P).

Council of defence of the doctoral thesis of Physical Sciences at Vilnius University:

Chairman:

Prof. habil. dr. Edmundas Kuokštis (Vilnius University, Physical Sciences, Physics – 02 P).

Members:

Prof. habil. dr. Jurgis Babonas (Institute of Semiconductor Physics of Center for Physical Sciences and Technology, Physical Sciences, Physics – 02 P).

Prof. dr. Aldona Beganskienė (Vilnius University, Physical Sciences, Chemistry – 03P).

Prof. habil. dr. Antanas Česnys (Vilnius Gediminas Technical University, Physical Sciences, Physics – 02 P).

Prof. habil. dr. Sigitas Tamulevičius (Kaunas University of Technology, Physical Sciences, Physics – 02 P).

Opponents:

Dr. Ramūnas Aleksiejūnas (Vilnius University, Physical Sciences, Physics – 02 P).

Dr. Šarūnas Meškinis (Kaunas University of Technology, Physical Sciences, Physics – 02 P).

The official defence of the doctoral thesis will be held in the public session of Physical Sciences at 3 p.m. on the 15th of October, 2010, in lecture room 212 at Faculty of Physics, Vilnius University, Saulėtekio av. 9-III, LT-10222 Vilnius, Lithuania.

Summary of the doctoral thesis has been distributed on the … of August, 2010.

The thesis is available at Vilnius University library and at the library of Institute of Physics of Center for Physical Sciences and Technology.

VILNIAUS UNIVERSITETAS,

FIZINIŲ IR TECHNOLOGIJOS MOKSLŲ CENTRO

FIZIKOS INSTITUTAS

Pranciškus Vitta

RELAKSACIJOS VYKSMŲ DAŽNINĖ SPEKTROSKOPIJA
OPTOELEKTRONIKOS MEDŽIAGOSE IR PRIETAISUOSE

Daktaro disertacijos santrauka
Fiziniai mokslai, fizika – 02 P

Vilnius, 2010

Disertacija rengta 2006-2010 metais Vilniaus universiteto Fizikos fakulteto Puslaidininkių fizikos katedroje bei Taikomųjų mokslų institute .

Mokslinis vadovas:

Prof. habil. dr. Artūras Žukauskas (Vilniaus universitetas, fiziniai mokslai, fizika – 02 P).

Konsultantas:

Prof. habil. dr. Gintautas Tamulaitis (Vilniaus universitetas, fiziniai mokslai, fizika – 02 P).

Disertacija ginama Vilniaus universiteto Fizikos mokslų krypties taryboje:

Pirmininkas:

Prof. habil. dr. Edmundas Kuokštis (Vilniaus universitetas, fiziniai mokslai, fizika – 02 P).

Nariai:

Prof. habil. dr. Jurgis Babonas (Fizinių ir technologijos mokslų centro Puslaidininkių fizikos institutas, fiziniai mokslai, fizika – 02 P).

Prof. dr. Aldona Beganskienė (Vilniaus universitetas, fiziniai mokslai, chemija – 03 P).

Prof. habil. dr. Antanas Česnys (Vilniaus Gedimino technikos universitetas, fiziniai mokslai, fizika – 02 P).

Prof. habil. dr. Sigitas Tamulevičius (Kauno technologijos universitetas, fiziniai mokslai, fizika – 02 P).

Oponentai:

Dr. Ramūnas Aleksiejūnas (Vilniaus universitetas, fiziniai mokslai, fizika – 02 P).

Dr. Šarūnas. Meškinis (Kauno technologijos universitetas, fiziniai mokslai, fizika – 02 P).

Disertacija bus ginama viešame Fizikos mokslo krypties posėdyje 2010 metais spalio 15 d. 15 valandą Vilniaus universiteto Fizikos fakulteto 212 auditorijoje, Saulėtekio al. 9-III, LT-10222 Vilnius, Lietuva

Disertacijos santrauka išsiuntinėta rugpjūčio … d., 2010 metais.

Disertaciją galima peržiūrėti Vilniaus universiteto ir Fizinių mokslų ir technologijų centro Fizikos instituto bibliotekose.

Santrauka

Pagrindinis disertacijos tikslas buvo sukurti, patobulinti ir realizuoti optoelektronikos medžiagų (organinių ir neorganinių puslaidininkių, fosforų) ir prietaisų (puslaidininkinių šviestukų) optinių, ir elektrinių parametrų dažninės skyros tyrimų metodikas, suteikiančias svarbios informacijos apie tiriamo objekto savybes ir sudarančias pagrindą tolimesniam tiriamų medžiagų tobulinimui bei technologinei plėtrai.

Disertacija yra sudaryta iš keturių skyrių, suskirstytų į smulkesnius skyrelius. Kiekvieno skyriaus išvados yra pateikiamos atitinkamo skyriaus gale, o visos disertacijos išvados yra pažymėtos disertacijos pabaigoje prieš cituojamos literatūros sąrašą. Bendras visiems skyriams naudotas literatūros sąrašas yra pateikiamas darbo pabaigoje. Disertacijos pradžioje yra disertanto kartu su bendraautoriais išpublikuotų publikacijų sąrašas (tiek įtrauktų, tiek neįtrauktų į disertaciją), ir šios publikacijos cituojamos tekste su priešdėliu „P", o konferencijų pranešimai su priešdėliu „K".

Pirmame skyriuje, sudarytame iš trijų poskyrių bei išvadų, yra pateikiama metodinė dažninės skyros matavimų medžiaga. Gesimo trukmės matavimo dažninės skyros metodu įprastinė teorija bei trumpa raidos istorija yra apžvelgiama pirmajame poskyryje. Antras poskyris yra skirtas puslaidininkiniu šviestuku sužadintos fotoliuminescencijos gesimo tyrimo schemai bei eigai, naudotoms daugumoje eksperimentų. Trečias pirmo skyriaus poskyris apžvelgia specifinį dažninės skyros fluorescencijos gesimo trukmės matavimo atvejį, kai registruojamame signale vyrauja sinfazinis fonas.

Antras disertacijos skyrius, sudarytas iš dviejų poskyrių, yra skirtas puslaidininkinių optoelektronikos medžiagų dažninei spektroskopijai. Pirmame skyrelyje yra apžvelgiami GaN epitaksinių sluoksnių ultravioletinės ir geltonosios liuminescencijos kinetiniai tyrimai itin silpno kvazitolydinio sužadinimo atveju. Antras poskyris yra skirtas dviejų tipų organinių puslaidininkių, galimai pritaikomų optoelektronikoje, PL gesimo dėsnių tyrimui dažniniu metodu. Čia yra pateikiami trijų konformacijų polisilano, įterpto į porėtą silicio oksidą, fluorescencijos ir TQL ligandų su iridžio kompleksais tiek fluorescencijos, tiek fosforescencijos gesimo dėsnių tyrimai.

Trečias skyrius yra skiriamas neorganiniams fosforams, kurie gali būti panaudoti bangos ilgio keitikliuose baltuose šviestukuose. Pirmame poskyryje yra pažvelgiami YAG:Ce fosforų emisijos rezultatai, priklausantys nuo cerio koncentracijos bei sintezės temperatūros. YMASG:Ce fosforo emisijos kvantinė išeiga ir gesimo trukmė, kaip funkcijos nuo cerio koncentracijos bei sintezės temperatūros, yra nagrinėjamos antrame poskyryje. Pastarojo tipo fosforų savybės yra palyginamos su YAG:Ce fosforo savybėmis.

Ketvirtame skyriuje yra apžvelgiamos prekinių puslaidininkinių šviestukų šiluminių savybių tyrimų metodikos ir jų rezultatai. Pirmame poskyryje yra pademonstruotas naujas tyrimo metodas, leidžiantis išmatuoti šviestuke sumontuotų fosforinių spinduliuotės keitiklių temperatūrą, matuojant fosforų emisijos gesimo trukmę. Šiame poskyryje yra detaliai pristatytos tiek eksperimento, tiek kalibravimo procedūros. Šviestukų šiluminių relaksacijos konstantų matavimo metodika yra pristatoma antrame skyrelyje. Šiluminių procesų dinaminiams tyrimams yra panaudojama gerai žinoma puslaidininkinio šviestuko tiesioginės įtampos priklausomybė nuo temperatūros. Yra parodoma, kad harmoniškai moduliuota srove maitinamo šviestuko įtampos fazės ir moduliacijos kreivės srovės atžvilgiu demonstruoja charakteringus linkius, žyminčius šiluminės relaksacijos konstantas.

Acknowledgement

List of abbreveations, used in the text

BPF   - band pass filter;

DAP   - donor-acceptor pair;

DM   - dichroic mirror;

EQE   - external quantum efficiency;

TQL   - triazole-quinoline ligand;

YAG   - yttrium aluminium garnet ($Y_3Al_5O_{12}$);

YMASG:Ce   - $Y_{3-x}Mg_2AlSi_2O_{12}:Ce_x^{3+}$ phosphor;

LED   - light-emitting diode

LPF   - long pass filter;

MLCT   - metal-to-ligand charge transfer;

MOCVD   - metal-organic chemical vapour deposition;

OLED   - organic light emitting devise;

PHOLED   - phosphorescent OLED;

PL   - photoluminescence;

PLED   - polymer light emitting devise;

SPF   - short pass filter;

WOLED   - white OLED.

Introduction

Recent globalisation and increased rate of world-wide energy consumption have brought up the semiconductor optoelectronics as promising solar energy (photovoltaic) and efficient lighting solution. Various scientific predictions state that widely-spread solid state lighting is capable not only to save a huge amount of energy and billions of dollars, but also to decrease the emission of CO_2 causing global-warming effect and other burning process contaminants such as SO_2, mercury, uranium etc. Furthermore, solid-state lighting is a new generation lighting technology, where functionality, controllability and colour versatility of lighting systems surpasses any known lighting solutions [1]. Often the invention of high brightness light-emitting diode is compared with the invention of semiconductor transistor which has pushed the revolution of modern electronics.

Despite the production of commercial high power LEDs on high scale, scientific interest in the field of optoelectronics is still present and a lot of topics still need attention. The efficiency and longevity of solid-state light sources are of primary importance. The characteristics (optical flux, spectra, efficiency, longevity and etc.) of a LED depend on the initial materials such as active semiconductor media, phosphor convertor, package components, as well as on temperature and other operating conditions. Therefore many scientific research techniques for the characterization of optoelectronic materials and already fabricated devices are being developed and attract much attention. In particular, laser-based spectroscopy techniques are well known and widely used for the investigation of optical properties of the materials, but the ability to apply LEDs instead of bulky and expensive lasers opens new research horizons.

Time- and frequency-domain photoluminescence decay investigation techniques are used for about 60 and 90 years respectively. These techniques in principle are equivalent and interconnected by the Fourier transform, but the operation of easily modulable LED in the frequency-domain measurements is more attractive, due to the quasi-continuous excitation with lower peak power and much higher integrated excitation energy. The pulsed excitation based systems has another drawback in that after the excitation pulse ends the measurement conditions (density of excited carriers, temperature, etc.) vary dramatically and the results of the measurements are difficult to interpret.

Keeping in mind the points mentioned above, the thesis was aimed to the frequency-domain measurement technology of modern optoelectronic materials and devices with further intention to apply the knowledge and experience in R&D applications.

Main goals

To design, develop and apply the techniques for the investigation of the optical and electrical parameters of optoelectronic materials and devices in the frequency domain. The investigation results are addressed for the further research and development of optoelectronic materials and devices.

Main objectives

To develop and test a measurement setup of visible or/and UV LED-excited PL decay times in the frequency domain with the requirements for the technique such as simplicity, single photodetector, wide range of measurable decay times and versatility in applications.

To develop a frequency domain PL decay time measurement technique with an admixed high level of in-phase background as an alternative for background-suppressed techniques. To motivate theoretically the operation principles and interpretation of the results.

To perform frequency-resolved PL decay time measurements in organic optoelectronic materials and inorganic phosphors, using LEDs for harmonically modulated excitation.

To perform an investigation of PL kinetics in GaN epitaxial layers under extremely low quasi-continuous UV-LED excitation.

To design and develop the investigation techniques operated in the frequency domain, for *in-situ* thermal characterization of encapsulated LEDs. To perform the measurements of the phosphor temperature and thermal relaxation constants in commercial high- and low-power LEDs.

Novelty and importance of the thesis

A technique of frequency resolved measurements in the presence of high level in-phase background was developed and theoretically validated.

GaN yellow and near-band-edge photoluminescence decay was investigated in the regime of extremely low ($2.5 \, \text{mW/cm}^2$) quasi-continuous excitation and wide temperature range (8-270 K).

PL decay measurements in the frequency domain were applied for novel and promising organic optoelectronics materials poly(di-n-hexylsilane) confined in nanoporous silica and phosphorescent bis-cyclometallated iridium complex based on triazole-quinoline ligand.

Integrated PL intensity and decay in promising YAG:Ce and YMASG:Ce phosphors synthesised by aqueous sol-gel combustion method were investigated as functions of annealing temperature and cerium content.

Novel LED thermal characterization techniques were developed and demonstrated for in-situ measurements of the phosphor temperature and thermal relaxation constants within the semiconductor chip in encapsulated LEDs.

The points to be maintained (statements to defend)

1. Frequency resolved PL signal phase measurements in the presence of high level of in-phase background are transformed into phase peak spectrum, where each decay component is represented by a height of the peak proportional to the fractional intensity and a peak position equal to inverse decay time.

2. Low temperature $(8 - 40\ K)$ decay of yellow luminescence in GaN epitaxial layer under quasi-continuous 2.5 mW/cm^2 excitation density demonstrates the partial recombination through DAP, similarly as in previously reported case of much powerful pulsed excitation $(10 - 10^4\ W/cm^2)$.

3. Quasi-continuously excited (under conditions similar to real LED operation mode) PL intensity of YAG:Ce phosphors synthesised by a sol-gel technique, is limited by the absorption in tail states of YAG crystal (in samples annealed at 1000° C) and by segregation of CeO_2 phase (in samples annealed at 1300° C) that optically effects the excitation and light extraction of microcrystallites.

4. The inorganic phosphor converters in high-power commercial LEDs investigated by frequency-resolved phosphor thermometry technique have the temperature that is lower than that of the semiconductor junction.

5. The forward voltage of harmonically modulated current driven LEDs has characteristic phase dips and modulation depth ramps at angular frequencies equal to the inverse thermal relaxation constants of the inner LED components. The thermal relaxation from active layer into the rest of the chip proceeds with the time constant as short as 1 ms, while the relaxation into the further LED parts takes as long as $10 - 160$ ms.

11

Layout of the thesis

The thesis is consisted of five chapters. The articles and conference contributions of the author together with co-authors are listed at the beginning of the thesis. The thesis is finalized by the concluding summary of all chapters. The layout of the chapters is organised as follows.

Chapter 1. PHOTOLUMINESCENCE LIFETIME MEASUREMENTS IN FREQUENCY DOMAIN.

1.1. Classical luminescence decay time measurement theory

The literature review of the history of term "luminescence" and evolution of the earliest PL decay measurements are presented in section 1.1. It is known that the PL intensity response function $I(t)$, which depends on the structure and environment of luminescent material, usually is expressed as single- or multi-exponential decays [2]

$$I(t) = \alpha \exp(-t/\tau) \text{ or } I(t) = \sum_i \alpha_i \exp(-t/\tau_i) , \tag{1}$$

respectively. Here α_i are the pre-exponential factors (also called as "contribution" or "zero-time intensity") of each fluorophore/residue having decay time τ_i. The term "fractional intensity" sometimes misused for α_i is calculated in such a way $k_i = \alpha_i \tau_i / \sum_i \alpha_i \tau_i$ and represents the contribution of decay component in integrated PL intensity. The luminescence decay law can be measured in time or frequency domains [2], which are related each to other through the Fourier transform. These two techniques are described in details and compared. The simplest single-exponent decay in time domain (Eq. 1a) has a following equivalent in the frequency domain

$$\tan\phi = \omega\tau \quad \text{and} \quad \mu = \left(1 + \omega^2\tau^2\right)^{-1/2} , \tag{2}$$

where ϕ is a phase shift and μ is demodulation factor of fluorescence signal in respect to the excitation waveform at an angular frequency $\omega = 2\pi v$. Here we can see that in the case of one-exponent decay, single frequency measurements can be performed.

1.2 Experimental setup of the PL decay law investigation in the frequency domain

The typical photoluminescence decay law measurement technique used in the majority of cases described in the thesis is depicted in Fig. 1. A sinus-shape signal is generated by a signal generator. A LED is driven by current bias admixed with the modulated current. The LED emission is collimated by a fused silica lens, passed through a SPF for cutting off the long-wavelength slope of the LED spectrum and directed to a dichroic mirror DM. The DM is designed to reflect the excitation beam and

to pass through the fluorescence signal of a longer wavelength. By a second fused silica lens, the reflected excitation is focused onto the sample, which can be of any form (powder, solution or solid) and fixed either in air atmosphere or in controlled temperature vacuum cryostat. The same lens is used to collect the outgoing photoluminescence and to guide it into the DM (transparent for PL). Further the PL signal is filtered by a BPF and/or monochromator to resolve the desired wavelength for the registration in a photomultiplier tube PMT. The electrical signal is spit into the AC and DC components by a second bias tee. The AC component is preamplified and fed into a lock-in amplifier, which performs the phase and modulation measurements employing cross-correlation technique. The experiment is controlled and data is collected by a PC operated by Labview® software.
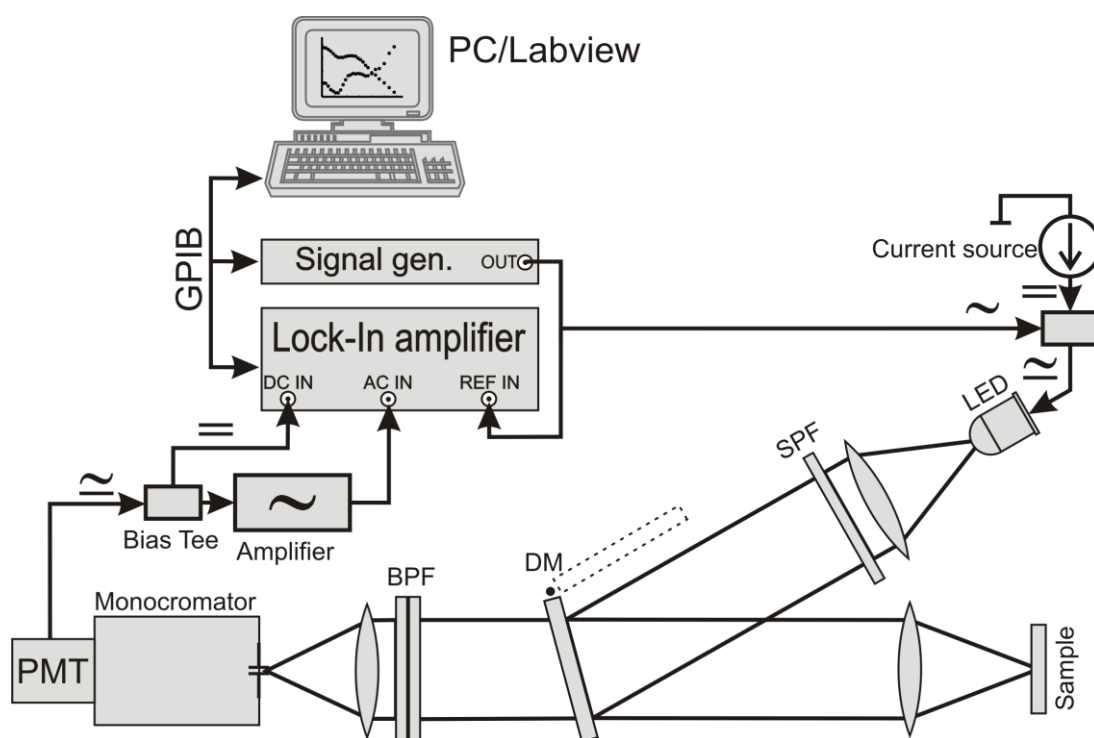
Fig. 1. Experimental setup of PL decay law measurements in the frequency domain.

### 1.3 Fluorescence lifetime measurements in the presence of high level in-phase background

One of the main drawbacks of the FD method is the lack of convenience in handling the measured data, since the fluorescence waveform phase and modulation frequency responses are much more difficult to interpret than conventional time response functions that are directly obtained in the time-domain measurement. Another drawback of the FD method is the in-phase background, which is due to incomplete optical isolation of the photodetector arm from the excitation one. In chapter 1.3, an alternative approach is proposed for handling the experimental frequency response of fluorescence

that is admixed with high levels of in-phase background. Differently from previous approaches based on removing or suppressing the background, here a use of a very high level of the background is made and shown that it allows a simple extraction of fluorescence lifetimes from the phase frequency response without sophisticated Fourier transformation and supplementary measurements.

It was theoretically demonstrated that mixing harmonically modulated fluorescence and excitation (in-phase background) signals results in sinus-shaped waveform with the phase shift and modulation depth expressed in such a way

$$\tan \Phi(\omega) = \frac{F_0 N_\omega}{F_0 D_\omega + B_0} \text{ and } M(\omega) = \frac{\sqrt{(F_0 D_\omega + B_0)^2 + (F_0 N_\omega)^2}}{F_0 + B_0} .$$ (3)

Here F_0 and B_0 are the steady-state (time-integrated) intensities of fluorescence and background respectively and N_ω and D_ω are the sine and cosine transforms used to convert the time domain data into the frequency domain [2]. In the limit of high in-phase background ($B_0 \gg F_0$), the spectrum of phase has peaks at angular frequencies equal to the inverse decay times of the decay components and the height of peaks represent the fractional intensities of those.
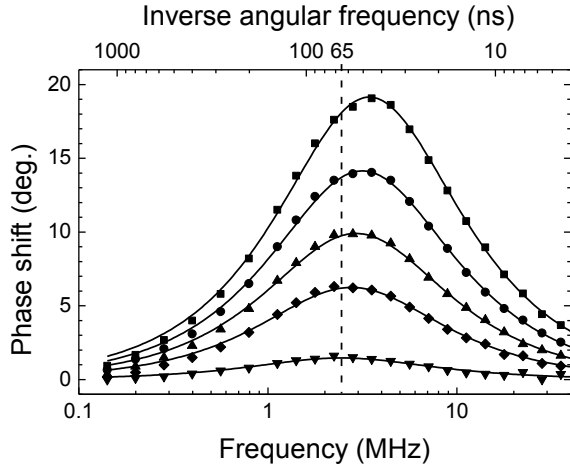
Fig. 2. Points, measured frequency response of phase shift for the monophospor LED in the presence of different levels of in-phase background (indicated). Solid lines, full theoretical fit according to Eq. (3). Dashed line depicts the inverse frequency value of 65 ns [P12].
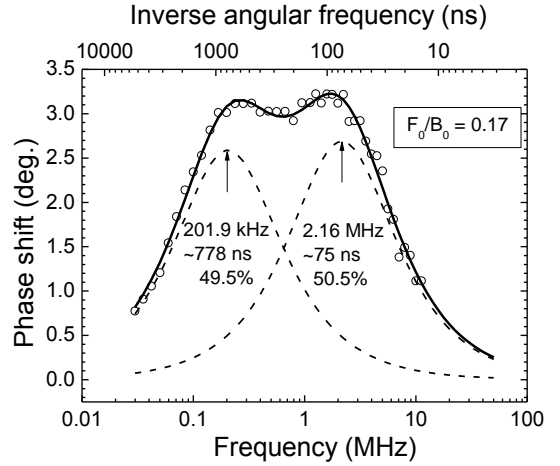
Fig. 3. Points, measured frequency response of the PL phase shift of the phosphor blend in a warm white LED in the presence of a high level of in-phase background. Dashed lines, calculated components of the sine transformation N_ω; solid line, sum of those [P12].

The introduced theoretical approach was demonstrated for phosphor emission decay time measurements in phosphor conversion white LEDs. The beam from a white LED containing both spectral components, blue semiconductor chip electroluminescence (excitation) and yellow phosphor PL, was geometrically split into two optical branches of different spectral transmission. The InGaN semiconductor chip emission spectral component served as excitation and in-phase background source. After filtering, these

14

two spectral beams (PL and in phase background) were mixed on frosted glass with controllable ratio.

The points in Fig. 2 depict the measured frequency response of fluorescence phase for the monophosphor LED with the in-phase background gradually introduced. With decreasing the F_0/B_0 ratio from 1 to 0.05, the peak of the phase vs. frequency dependence shifts to lower frequencies and the magnitude of the peak decreases as predicted by Eq. (3) (lines in Fig. 2). At very low F_0/B_0 ratios, the peak is seen to approach an inverse angular frequency of about 65 ns, which is the value extracted from the frequency response in the absence of in-phase background.

The points in Fig. 3 show the measured phase shift as a function of frequency for phosphor blend fluorescence of a warm white LED in the presence of high in-phase background (fluorescence-to-background ratio of 0.17). The measured dependence exhibits two distinct peaks corresponding to fluorescence lifetimes of the two phosphors. A simple decomposition of the phase dependence into two components of the sine transformation N_ω (in Fig. 3) yields the decay time values of 778 ns and 75 ns, respectively, which are in fair agreement with those obtained from the analysis of the phase response with suppressed background (not shown here). The solid line in Fig. 3 shows the sum of the components.

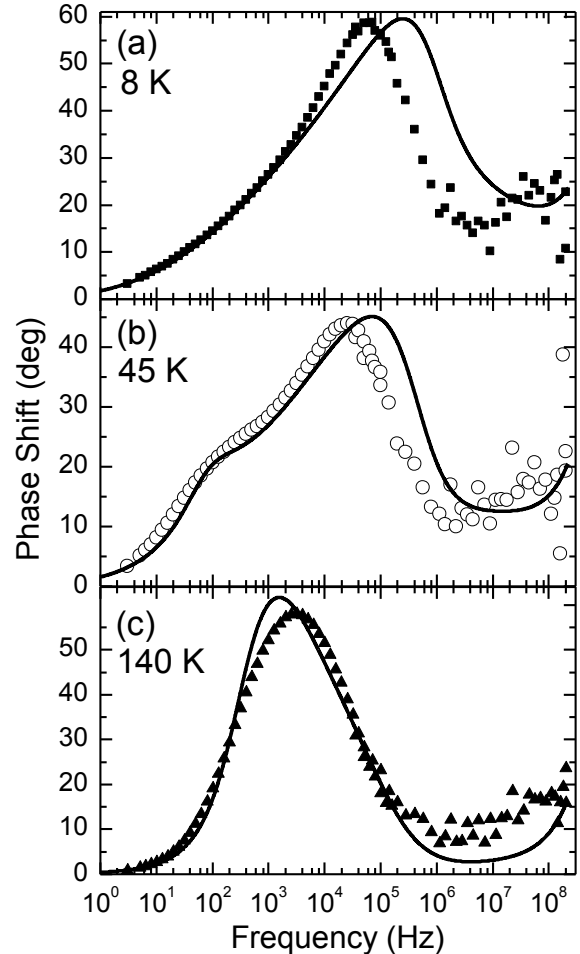**Chapter 2.** INVESTIGATION OF SEMICONDUCTING OPTOELECTRONIC MATERIALS

2.1 Frequency resolved PL decay measurement in GaN epilayers

To study the photoluminescence kinetics at extremely low carrier densities, fluorescence lifetime measurements in the frequency domain were employed [2]. This technique also enabled us to expand the time scale of the PL decay study to long lifetimes up to milliseconds. A 280 nm LED from Sensor Electronic Technology, Inc. was used as an excitation source in the frequency-domain PL decay measurement experiments. The LED emission intensity and, hence, the PL signal, were modulated in the frequency range from 5 Hz to 200 MHz. The experiment setup was similar to one depicted in Fig. 1 and the time evolution was extracted using Fourier-transform analysis. The samples were grown by migration-enhanced MOCVD technique in Sensor Electronic Technology, Inc (USA).

Two spectral regions recognized as yellow and near-band-edge (NBE) luminescence were studied separately. The spectral resolution was maintained by selecting proper band-pass filters. The phase shift curves of the NBE luminescence (not shown), which also included recombination via excitonic states, had two features in the entire temperature range and were fitted by the superposition of two exponential decay functions with decay times of ~176 μs and 200 ps.

Three temperature-dependent components were observed in the yellow luminescence decay (Fig. 4). The phase shift increase in the 5 Hz to 30 kHz range observed at temperatures below ~40 K was too slow to be described by an exponential decay. Thus, it was assumed that this feature was caused by donor–acceptor pair (DAP) recombination, which had previously been observed in GaN [3, 4] and proceeded at the rate, determined by the distance between the donor and acceptor involved [5]. To reproduce the drop in the phase shift in the high-frequency limit (Fig. 4a), a fast exponential decay component with decay time of 200 ps (similar to NBE luminescence) was included into the fitting function. This decay component, which might be even faster than 200 ps, persisted throughout the entire temperature range under study. At elevated temperatures, a new exponential decay component emerged (Fig. 4b). Its decay time decreased from ~10 ms at 30 K to ~500 μs at 100 K. Above 100 K, the

Fig. 4. Phase shift frequency dependence of the YL band in GaN (points) for three typical temperatures (indicated). The solid lines show the best fit curves. [P5]

yellow PL kinetics showed no significant change and exponential component with $\tau = 500$ μs dominated over the DAP recombination component (see Fig. 4c). It is reasonable to assume that this component is caused by optical transitions between the conduction band and acceptors. It replaced the DAP recombination when the donor states involved in DAP recombination became thermally ionized.

In conclusion, the fluorescence decay time measurement in the frequency domain enabled us to perform the study at an extremely low excitation power density (~2.5 mW/cm^2) and to reveal the competition between recombination mechanisms responsible for yellow luminescence in GaN at nonequilibrium carrier densities below the saturation of the energy levels involved in these recombination channels.

2.2 Investigation of organic optoelectronic materials

2.2.1 Temperature independent exciton relaxation in poly(di-n-hexylsilane) confined in nanoporous silica

Luminescence external quantum efficiency (EQE) and exciton lifetimes in different forms of poly(di-n-hexylsilane) (PDHS) confined within silica pores of 10-nm diameter were studied at different temperatures. The samples were prepared by partners at Institute of Physics of Centre for Physical Sciences and Technology. The luminescence EQE was estimated using an integrating sphere coupled to a CCD spectrometer at 365-nm excitation by a UV LED. The technique used for the estimation of EQE was similar to that described in Ref. 6. The PL kinetics has been defined by analyzing the luminescence signal phase shift and the modulation amplitude in the frequency range from 100 kHz to 200 MHz. A harmonically modulated deep-UV LED with the peak emission at 280 nm was used as the excitation source and the experiment was carried out using a setup similar to that shown in Fig. 1.
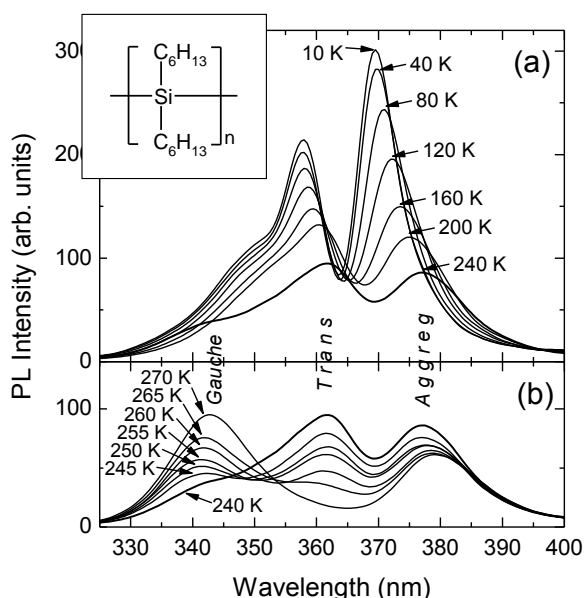
Fig. 5. PL spectra of PDHS confined within 10-nm size pores of nanoporous silica as a function of temperature, measured in the range of (a) 10–240 K with an increment of 40 K and (b) 240–270 K with an increment of 5 K. The structural formula of PDHS is presented in the inset [P7].
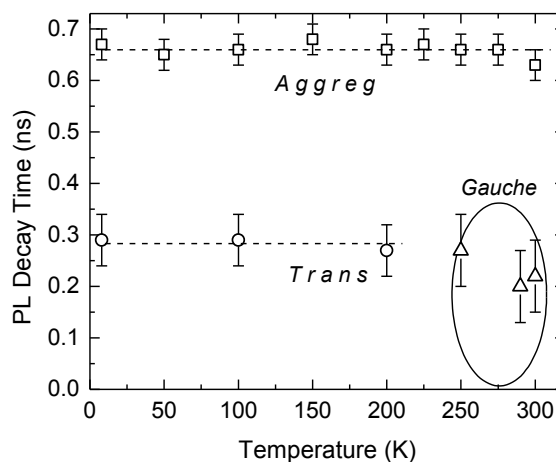
Fig. 6. Temperature dependence of the dominant PL decay time (fractional intensity >93%) in *trans*- and *gauche*-conformations and aggregate states of PDHS. The dashed lines are guides for the eye [P7].

The PL spectrum variation with temperature for PDHS embedded in the SBA-15 nanopores of 10-nm size measured by slowly heating the sample from 10 K to 270 K is shown in Fig. 5. Basing on earlier study [7], two well-resolved narrow bands peaking at 358 nm and 370 nm with the full width at half magnitude (FWHM) of about 8 nm at 10 K were attributed to the ordered *trans*-conformers and aggregate states, respectively. The broad band with FWHM of ~ 16 nm located far most in the UV region (at 342 nm)

and observed only above 240 K, i.e. after the onset of the *trans–gauche* thermochromic transition [7], was assigned to the disordered *gauche*-conformers. The thermochromic transition from *trans* to *gauche* form in PDHS is completed at about 270 K.

To reveal differences in the exciton relaxation between randomly oriented polysilane chains in films or solutions [7] and those aligned in nanopores and to gain a better understanding of the processes governing the temperature activated PL quenching of polysilanes confined in nanopores, the PL decay kinetics as a functions of temperature were studied. It was proposed that the luminescence lifetimes of the aggregate states and of the *trans*-conformation of PDHS confined in nanopores, were found to be independent of temperature within the experimental accuracy in the range of 10–300 K and 10–200 K, respectively (Fig. 6). This implies a constant luminescence EQE, and consequently, the temperature independent nonradiative decay rates within the accuracy of at least 18% for *trans*-conformation and 5% for aggregate states, respectively. Consequently, this finding indicates strong suppression of nonradiative decay channels and the absence of a thermally activated PL quenching of polysilanes embedded in nanopores, what is in contradiction with the results obtained for polysilane films and solutions [8, 9].

In conclusion, luminescence relaxation kinetics of different forms of PDHS confined within 10-nm size silica pores revealed the temperature independent exciton lifetimes for *trans* (0.28 ns) and aggregate states (0.66 ns), thus indicating the thermal stability of luminescence quantum yield and nonradiative relaxation rate. The absence of the temperature-enhanced nonradiative relaxation is favourable for the development of nanosized polysilane based optoelectronic devices, such as OLEDs. The successful realization of such polymer-in-nanopore based electrically pumped light-emitting devices could provide superior thermal stability and operation performance.

2.2.2 Investigation of phosphorescent iridium complex based on triazole-quinoline ligand

The samples were synthesized in the Faculty of Chemical Technology of the Kaunas University of Technology. Photoluminescence spectra of bis-cyclometallated iridium (III) complex and a free ligand used in its synthesis were measured using a double monochromator coupled to a photomultiplier operating in the photon-counting mode. PL lifetimes were measured in the frequency domain (0.1–100 MHz) as described in section 1.2. The PL measurements were carried out at room temperature in dilute dimethyl sulfoxide (DMSO) solutions, which were continuously bubbled with high purity helium to remove dissolved oxygen and, thus, to avoid quenching of the radiative decay from the triplet states.

The PL spectrum of helium degassed DMSO solutions of iridium complex with phenyltriazole-quinoline-based ligand is depicted by the solid line in Fig. 7. For

comparison, the spectra of air saturated solution of bis-cyclometallated iridium complex (dashed line) and pure TQL (dotted line) are also displayed. The emission lifetimes of the two PL bands, i.e. ligand-based band and that related to triplet MLCT excited state, are shown in Fig. 8. The decay times were determined by measuring frequency dependences of phase shift (open points) and modulation ratio (solid points) at the band peaks. The measured frequency responses for free phenyltriazole-quinoline-based ligand and bis-cyclometallated iridium complex are depicted in Figs. 8(a) and (b), respectively. The lifetimes were extracted by fitting the experimental data with the single- and two-exponent decay laws.
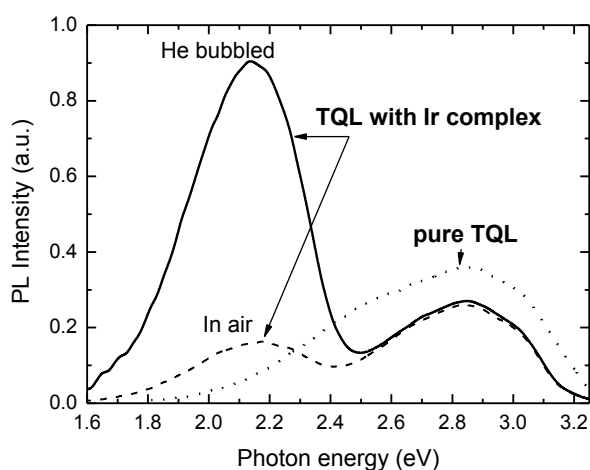
Fig. 7. Room temperature PL spectra of DMSO solutions (10^{-4} M) of biscyclometallated iridium complex (solid and dashed lines) and pure phenyltriazole-quinoline-based ligand (dotted line). Solid line, helium degassed solution [P8].
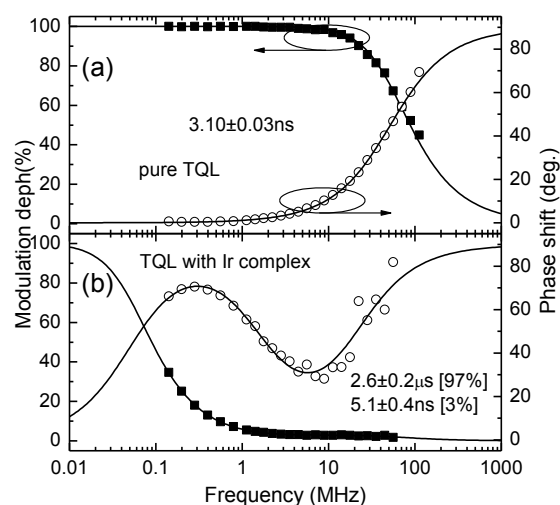
Fig. 8. PL phase shift (open points) and modulation ratio (solid points) as a function of modulation frequency in helium degassed DMSO solutions of pheny-ltriazole-quinoline based ligand (a) and bis-cyclometallated iridium complex (b). The lines correspond to single (a) and double-exponential (b) decay modelling of the data with the characteristic lifetimes τ indicated [P8].

The observed features support the dominant MLCT nature of the excited triplet states involved in the transition, which is known to be partly allowed due to strong spin–orbit coupling of the 5d electrons of iridium. The revealed properties along with the high phosphorescence quantum yield (78%) implies the new bis-cyclometallated iridium(III) complex, based on the novel triazole-quinoline ligand, as an efficient yellow triplet-emitter for OLEDs.

19

Chapter 3. INVESTIGATION OF INORGANIC PHOSPHORS USED AS WAVELENGTH CONVERTERS IN WHITE LEDS.

### 3.1 Aqueous sol-gel synthesised YAG:Ce phosphors

The present section is focused on the optimization of sol–gel technology for the fabrication of YAG:Ce phosphors for white LEDs. The sinterability and physical properties of sol-gel-derived cerium-activated yttrium aluminium garnet samples ($Y_3Al_5O_{12}$:Ce), synthesized at Chemistry Department in Vilnius University, were investigated as functions of final annealing temperature (1000 and 1300 °C) and dopant concentration (up to 10 mol% of Ce).

PL spectra of all samples were measured under identical conditions using a LED with the emission band peaked at 440 nm as an excitation source. The spectra were recorded by a double monochromator and a photomultiplier operating in the photon counting mode. In the frequency-domain fluorescence lifetime measurements, the output of the 440-nm LED was modulated within the frequency range from 50 kHz to 200 MHz. The PL decay measurement data was fitted by a two-exponent decay law.

The integrated PL intensity showed a nonmonotonic dependence on Ce concentration (Fig. 9). In the set of YAG:Ce samples sintered at 1000 °C, PL intensity (open points) slightly increased with increasing Ce
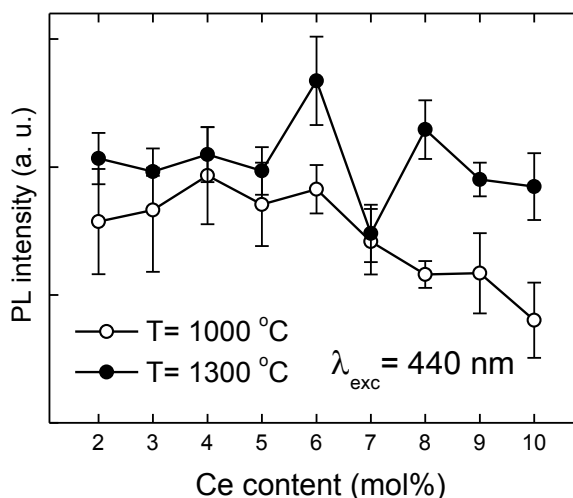
Fig. 9. Dependences of spectrally integrated PL intensity on Ce content for YAG:Ce samples annealed at 1000 °C (open points) and 1300 °C (filled points) for excitation wavelength of 440 nm [P3].
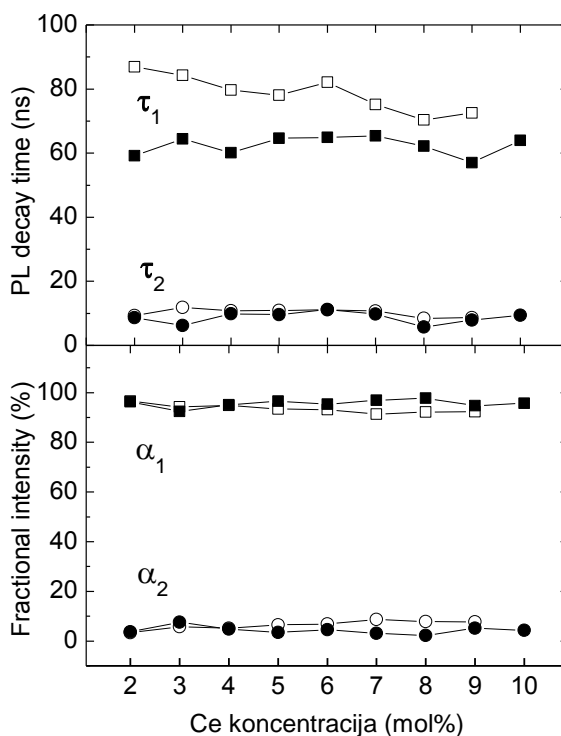
Fig 10. Two photoluminescence decay times (τ_1, τ_2) and corresponding weight coefficients of the exponential decay components (α_1, α_2) for samples synthesized at 1000 °C (open shapes) and 1300 °C (closed shapes) as a function of Ce concentration [P3].

content up to ~4% and dropped down by a factor of 1.5 with the further increase of Ce content up to 10%. Meanwhile, the PL intensity dependence on Ce content in the set of samples sintered at 1300 °C (solid points) exhibited different behaviour. The intensity was almost constant up to the Ce content of ~5%. However, in the samples with Ce concentration higher than 5% we observed strong irregular bounces of the PL intensity. Note that the bouncing was observed in samples that exhibited crystalline oxide CeO_2 as a separate phase in the x-ray diffraction spectra (XRD) [P3].

The summary of the fluorescence lifetime measurement results is presented in Fig. 10. Both the decay time and relative intensity of the short decay component were constant in all samples irrespective of Ce content and sintering temperature. Meanwhile, the variation of the longer decay time exhibited sensitivity to sintering temperature. In the set of samples sintered at 1300 °C, the decay time did not depend on Ce content and was equal to ~60 ns. The decay time in the set of samples sintered at 1000 °C was somewhat longer and exhibited a slight decrease with Ce content. The decay constant τ_1 equalled ~90 ns in the sample with 2% of cerium and almost linearly declined down to ~70 ns in the sample with 10% of Ce. These lifetimes were much higher than a value of 30 ns previously reported for sol–gel fabricated YAG:Ce micro crystals [10] and is in the range of typical fluorescence decay times in single-crystal and ceramic YAGA:Ce (60–90 ns) [11].

Heat treatment of mixed-metal chelates at relatively low temperatures (1000 °C) yielded monophasic homogeneously Ce-doped crystalline YAG with up to 10 mol% of Ce. However, such a low sintering temperature resulted in a strong concentration quenching, probably, due to the optical losses in the tail states of the doped YAG lattice and some nonradiative energy transfer from the excited activator ions. The synthesis of YAG:Ce at a higher temperature of 1300 °C resulted in an increased PL output and reduced concentration quenching (almost no quenching was observed for long-wavelength 440-nm excitation). However, with increasing Ce content above 4 mol%, large fluctuations of PL output were observed. These fluctuations were tentatively attributed to unstable conditions for the excitation of the activator ions and escape of the resulting PL, possibly, due to the formation of the secondary CeO_2 phase, which was evidenced by XRD.

3.2 Aqueous sol-gel synthesised YMASG:Ce phosphors

The investigation of an efficient red phosphor $Y_{3-x}Mg_2AlSi_2O_{12}:Ce_x^{3+}$ (YMASG:Ce) with a charge-balanced composition and stable garnet phase is introduced in section 3.2. YMASG:Ce was fabricated using sol–gel combustion technique at institute of Applied research (Muenster, Germany). Effects of sintering temperature and Ce content on photoluminescence properties of the phosphor under blue LED excitation

are reported. The YMASG:Ce samples were with different Ce^{3+} content (0.015, 0.03, 0.045, and 0.06) and synthesized at different temperatures (1400, 1450, 1500 and 1550 °C) by sol–gel combustion method. The optical characterization techniques, including PL spectra and decay times measurements, were similar to those described in section 3.1. The PL external quantum efficiency measurements were performed by the integrating sphere method.

Figure 11 displays the normalized PL spectra of $Y_{3-x}Mg_2AlSi_2O_{12}:Ce_x^{3+}$ samples with different Ce content x (1550° C annealing temperature; the corresponding sets of samples annealed at lower temperatures down to 1400° C show the same trends.). The corresponding spectrum of the sol–gel derived YAG:Ce sample [P3] is also shown in Fig. 11 for comparison. The striking feature of the YMASG:Ce emission is a remarkable red shift of the band by ~50 nm in respect to that of YAG:Ce.
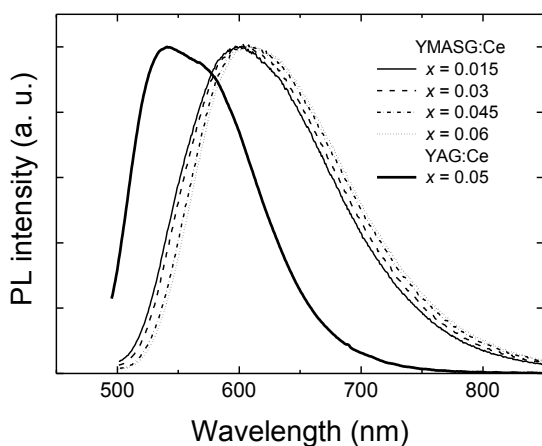
Fig. 11. Normalized PL spectra of $Y_{3-x}Ce_xMg_2AlSi_2O_{12}$ phosphors with different Ce content (indicated) annealed at 1550° C and PL spectrum of YAG:Ce with 5% of cerium [P11].
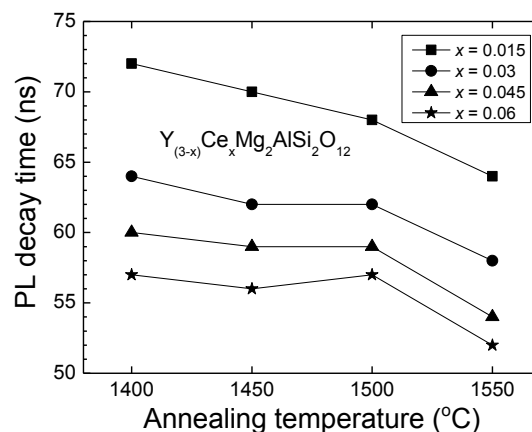
Fig. 12. Decay time of the slower PL component of $Y_{3-x}Ce_xMg_2AlSi_2O_{12}$ as a function of cerium content x and annealing temperature [P11].

The frequency response of the modulation depth and phase of YMASG:Ce PL were fitted by two-exponent decay law with dominating 50-75 ns component as well as with weak (~5% of fractional intensity) and relatively fast (5-8 ns) decay moiety. The slower decay component, which is probably due to allowed 5d–4f transitions, exhibited a dependence on Ce content and annealing temperature (Fig. 12) with the decay time constants typical of single-crystal, ceramic and microcrystalline YAG:Ce [10-12]. The decay time and EQE (not shown) decreased with increasing Ce content due to concentration quenching. Characterization

In conclusion, the $Y_{3-x}Ce_xMg_2AlSi_2O_{12}$ phosphor exhibited a PL band peaked at about 600 nm with a record red shift for cation-substituted YAG:Ce. The chromaticity coordinates of the YMASG:Ce phosphors are suitable for generating warm-white light (CCT = 3000 K) through blending with a blue component at about 483 nm. The emission

intensity and the fluorescence decay characteristics of the YMASG:Ce phosphors are similar to those of YAG:Ce, what implies that such warm-white LEDs can have efficiency comparable to that of the conventional daylight dichromatic LEDs.

Chapter 4. THERMAL CHARACTERIZATION OF COMMERCIAL LIGHT-EMITTING DIODES

4.1 White LED contained phosphor thermometry

In this section, a method for *in situ* measurement of phosphor temperature in commercial high-power white LEDs using phosphor thermometry is reported. The fluorescence decay time of the phosphor converter was employed as a temperature sensitive parameter to perform indirect temperature measurements. Fluorescence decay time was estimated using the frequency-domain technique based on direct high-frequency modulation of the LED driving current and measuring the phase shift of the resulting phosphor emission waveform in respect of that of the semiconductor chip. Two types of PHILIPS LUMILEDS LIGHTING high-power white LEDs were investigated. A high-operation-temperature "cool-white" LXK2-PW14 LED, which contains single standard YAG: Ce phosphor, was studied in a wide range of the mount temperature (up to 480 K). To demonstrate the thermometry in a phosphor blend, a "warm-white" LXHL-BW03 LED which contains YAG:Ce and a red phosphor, was examined in the temperature range up to 420 K.
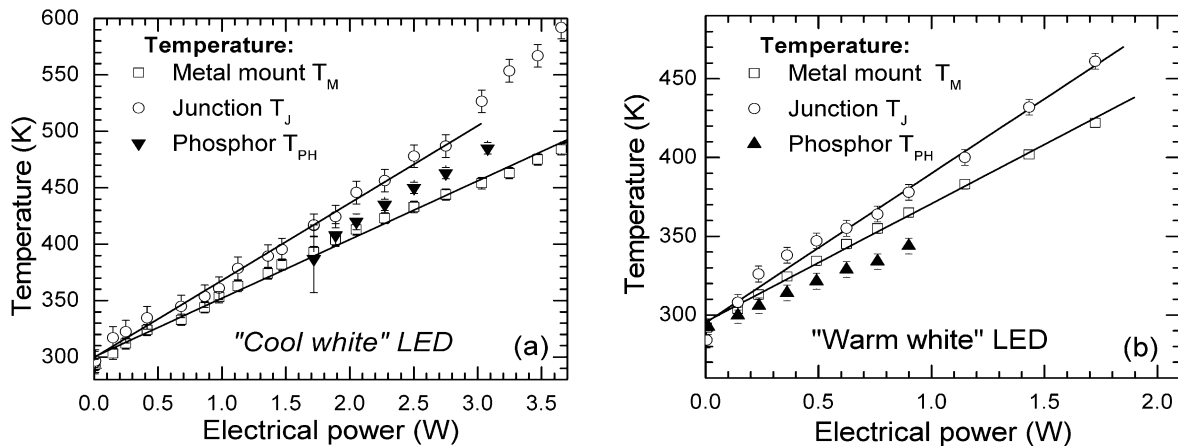
Fig. 13. Temperatures of the metal mount (squares), junction (circles), and phosphor (triangles) as functions of driving power in (a) "cool-white" and (b) "warm white" high-power LEDs. The lines are guides for the eye [P4].

The temperature of the metal mount (T_M) of the LED was measured by a thermocouple gauge with the accuracy of 1 K, whereas the temperature of the junction was estimated from the high-energy slope of the electroluminescence spectra. First, for

calibration purposes, the LEDs were disassembled and the silicone film containing phosphor particles was removed from the chip. The film was mounted on the brass finger of cryostat and fastened by a brass plate with a pinhole. The PL decay time dependences on temperature were measured for both types of LED phosphor converters. The phosphor blends were excited by a blue LED (LUMILEDS LXHL-LR5C), having emission similar to the short-wavelength emission of investigated LEDs and the measurements were performed in the frequency domain configuration. In the "coolwhite" phosphor, a single fluorescence lifetime was measured with a high accuracy (0.4%) and equalled about 63 ns up to 380 K with further decrease to about 53 ns at 485 K. Of two fluorescence lifetimes in the "warm-white" phosphor blend, one was close to that observed in YAG:Ce, whereas the second one monotonically decreased with temperature. The room-temperature value of this lifetime was 720 ns and it dropped to 350 ns at 352 K. Such a calibration data allowed for the estimation of the "cool white" and "warm white" phosphor temperature in the range of $380 - 485$ K and $293 - 530$ ns, respectively. The investigated LEDs were thermally isolated and the metal mount and junction temperatures as well as phosphor PL decay times (e.g. temperature) were investigated as functions of driving power (Fig. 13). The monophosphor in the "cool white" LED showed to have a temperature lower than that of the junction, but higher than the metal mount, while the temperature of the phosphor in the "warm white" LED was even lower than that of the metal mount, owing to spatial separation of phosphor converter from semiconductor chip.

In conclusion, we employed the dependence of phosphor fluorescence lifetime on temperature for the *in situ* characterization of the phosphor thermal condition in high-power white LEDs, which were directly modulated by high-frequency driving current. Phosphor temperatures within the typical error of about 5 K were measured as a function of driving power in LEDs containing a single phosphor and a phosphor blend. The phosphor temperature turned out to be lower than that of the LED junction, indicating on a temperature gradient inside the LED packages.

4.2 Frequency-resolved investigation of temperature dynamics inside the LED package.

In this section a method for measurement of LED thermal relaxation time constants in the frequency domain is reported. The temperature-sensitive characteristic employed in this method is the LED forward voltage.

Consider a LED driven by a forward current $I(t) = I_0(1 + m\sin\omega t)$ modulated at a frequency ω with a bias I_0 and modulation depth m. At frequencies that are much lower than the cut-off frequency of the LED, the forward voltage across the LED is given by

$$V(t) = V_0 + mI_0R_D \sin(\omega t) + m\frac{\partial V}{\partial T_J}\Delta T_J \mu(\omega)\sin[\omega t + \phi(\omega)], \tag{4}$$

where V_0 is the steady-state forward voltage at the driving current I_0, R_D is the dynamic resistance, $\partial V/\partial T_J$ is the temperature coefficient of the forward voltage, ΔT_J is the steady-state excess junction temperature, and $\mu(\omega)$ and $\varphi(\omega)$ are the modulation factor and the phase shift of the harmonically modulated junction temperature, respectively. Provided that the dynamic resistance is low enough ($R_D \ll V_0/I_0$), the heat generation rate in the junction almost follows the forward current variation. Assuming the temperature inside the chip to decay as a multi-exponent function, the measured forward voltage can be expressed as $V(t) = V_0 + U(\omega)sin[\omega t - \Phi(\omega)]$, where

$$U(\omega) = m\left(I_0R_D + \frac{\partial V}{\partial T_J}\Delta T_J D_\omega\right) \text{ and } \Phi(\omega) = m\frac{\partial V}{\partial T_J}\Delta T_J N_\omega \tag{5}$$

are the amplitude and the phase shift of the forward voltage in respect to current, respectively (N_ω and D_ω are the sine and cosine transformations, see Ref. 2.). When measured as functions of frequency, $U(\omega)$ and $\Phi(\omega)$ have ramps and dips, respectively, at the angular frequencies equal to inverted thermal relaxation constants.

The LEDs were driven using an operational amplifier based current source with a current measurement resistor connected in series with the LED. The bias equalled the nominal current (20 mA for low-power LEDs and 350 mA for high-power LEDs) and the current was slightly modulated by a harmonic signal ($m\sim10$). A digital lock-in amplifier was used for both generating the modulation signal and measuring the amplitude and phase of the forward voltage in respect of forward current (voltage across the measurement resistor) of the LED.

Figure 14 depicts the experimental data (points) and theoretical fits for common low-power LEDs in T1 package. Figures 1(a) and 1(b) present the measured frequency dependences of the phase shift between the driving voltage and current for a *p-n* junction GaP LED and for a double-heterostructure (DH) AlGaAs LED, respectively. At very low frequencies, both LEDs exhibited a drop in the phase shift in the 100 ms range, which can be attributed to thermal relaxation of the chip with respect to the metal lead (cup) that serves as a heat sink. Besides, the spectrum of the DH AlGaAs LED had a remarkable phase dip at a frequency of about 40 Hz that corresponds to a thermal time constant of 4 ms. The corresponding thermal relaxation route was attributed to the downward heat flow from the thin active layer to the rest of the chip (substrate). The measured frequency dependences of the forward voltage modulation amplitude were in line with the phase dependences (Fig. 14c).
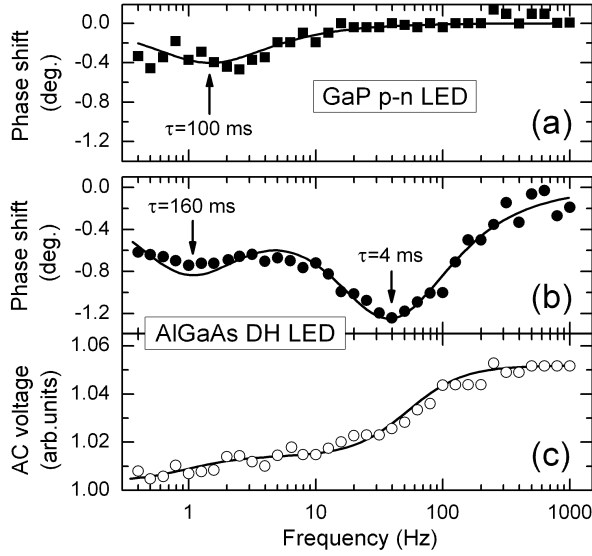
Fig. 14. Frequency dependence of the forward voltage *vs.* current phase shift in (a) a low-power (T1) *p-n* GaP LED and (b) a DH AlGaAs LED. (c) Frequency dependence of the forward voltage modulation amplitude in the AlGaInP LED. Points, experiment; lines, data fits to one-exponent (*p-n* GaP LED) and two-exponent (DH AlGaAs LED) thermal relaxation models, respectively, with the time constants indicated [P9].
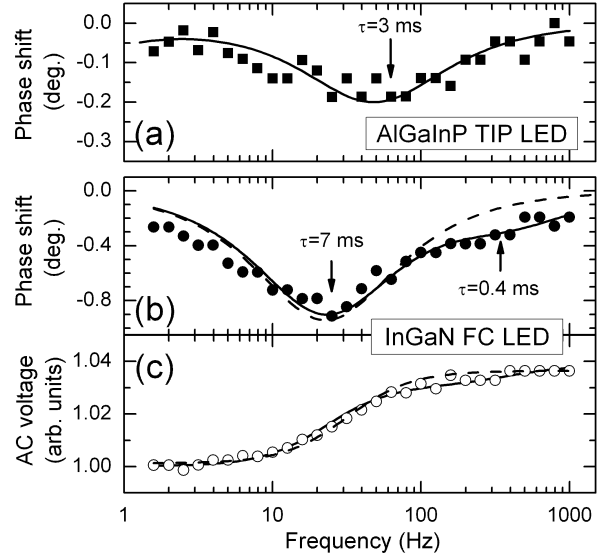
Fig. 15. Frequency dependence of the forward voltage *vs.* current phase shift in (a) a high-power TIP AlGaInP LED and (b) a FC InGaN LED. (c) Frequency dependence of the forward voltage modulation amplitude in the InGaN LED. Points, experiment; solid lines, data fits to one-exponent (TIP AlGaInP LED) and two-exponent (FC InGaN LED) thermal relaxation models, respectively, with the time constants indicated. Dashed lines, a single-exponent model for the FC InGaN LED [P9].

Figure 15 shows the results for high-power LEDs. A truncated-inverted-pyramid (TIP) AlGaInP LED [13] exhibited a week phase feature at about 50 Hz that corresponded to a thermal time constant of 3 ms (Fig. 15a). A flip-chip (FC) InGaN LED [14] had a prominent phase feature at about 23 Hz that corresponded to a thermal time constant of 7 ms (Fig. 15b). Also, a weak dip at about 400 Hz ($\tau = 0.4$ ms) can be resolved (the solid and dashed lines in Fig. 15b show a two-exponent and single-exponent fits, respectively). Figure 15c shows the voltage modulation amplitude spectrum for the FC InGaN LED with the corresponding ramps. The weak features in the spectra of the high-power LEDs (3 ms and 0.4 ms for the TIP AlGaInP LED and FC InGaN LED, respectively) are to be attributed to upward heat flows in the LED chips, which contain massive components on top of the active layers, a 200 μm thick GaP wafer-bonded pyramid base in the AlGaInP LED [13] and a 80 μm thick sapphire substrate in the InGaN LED [14], respectively. Meanwhile, the main 7-ms feature in the FC InGaN spectrum (Fig. 15b) can be attributed to a Si submount, which the heat flows from the active layer to the metal slug through [14].

The above assignments of the measured thermal time constants to heat flows were collated with numerical estimations in the steady-state regime. The steady-state thermal time constants of a thin heat-conductive slab in the one-dimensional problem were

estimated as $\tau = c\rho L^2/\kappa$, where c, ρ, κ, and L are the specific heat, density, thermal conductivity, and thickness the slab.

In conclusion, was developed a spectroscopic approach for the thermal characterization of LEDs based on the measurement of the frequency dependence of the forward voltage versus current phase shift. Thermal relaxation time constants were determined as inverse angular frequencies of the dips in the phase-shift spectrum. Such an approach can be useful for the analysis of transient self-heating within LEDs.

Conclusions of the thesis

1.   The presence of a high level of in-phase background in the frequency domain PL decay time measurements converts the phase curves into the spectra of decay components. The phase peak height is proportional to the decay component fractional intensity, while the peak position is at the angular frequency equal to the inverse decay time. Such an approach was demonstrated for the measurement of decay times of inorganic phosphor wavelength converters in "cool" and "warm" white LEDs. The measured decay times of 65 ns and 778 ns together with 75 ns long decay times in the "cool white" LED YAG:Ce phosphor and in the phosphor blend of "warm white" LED, respectively, fairly agreed with the values found in the literature as well as with the results obtained by conventional background suppressed frequency-resolved measurement technique.

2.   The technique of frequency resolved PL kinetics investigation under extremely low quasi-continuous UV LED excitation was realised for a GaN epitaxial layer. The measured decay shape of GaN yellow luminescence at a low temperature (8-40 K) exhibited strongly nonexponential decay due to partial recombination through DAP. The characteristic parameters of DAP recombination were resolved, and GaN band diagram was proposed.

3.   The investigation of PL decay and EQE of poly(di-n-hexylsilane) confined in nanoporous silica revealed the suppression of thermally activated non-radiative recombination in poly(di-n-hexylsilane) due to the confinement into the silica nanopores. All three conformations of poly(di-n-hexylsilane) (*Gauche*, *Trans* and *Aggreg.*) exhibited constant decay times within the experimental accuracy in entire range of temperatures applied (8-270 K).

4.   The frequency-domain PL investigation technique was applied for the decay measurements of both the phosphorescence and fluorescence in bis-cyclometallated iridium complex based on triazole-quinoline ligand. The measured decay times of 2.6 µs and ~5 ns for phosphorescence and luminescence, respectively, as well as record EQE (78 %) proved the recombination through the MLCT states in helium bubbled samples.

5. The investigation of the PL decay and integrated intensity of YAG:Ce phosphors synthesized by sol-gel combustion method, revealed that in samples annealed at 1000 °C, the activator (Ce^{3+}) PL decays are slightly effected by concentration quenching and integrated PL intensity is lowered due to the absorption in the tail states of YAG crystal, while the formation of separate CeO_2 phase was present in samples annealed at 1300 °C.

6. The frequency-domain PL investigation technique as well as EQE measurements proved a strong concentration quenching in YMASG:Ce phosphors synthesized by aqueous sol-gel combustion method.

7. The measurement technique employing the dependence of phosphor PL decay on temperature was designed and demonstrated for the *in situ* characterization of the phosphor thermal condition in high-power white LEDs that were directly modulated by high-frequency driving current. Phosphor temperatures within the typical error of about 5 K were measured as functions of driving power in LEDs containing a single phosphor and a phosphor blend. Phosphor temperature turned out to be lower than that of the LED junction, indicating on a temperature gradient inside the LED packages.

8. A spectroscopical approach for thermal characterization of LEDs based on the measurement of the frequency dependence of the forward voltage versus current phase shift was introduced. Thermal relaxation time constants were determined as the inverse angular frequencies of the dips in the phase-shift spectrum and revealed that thermal equilibrium inside the LED chip is achieved within the time of less than 1 ms, while the heat propagation into further LED components takes as long as 10-160 ms.

References

[1] E. Fred Schubert, Jong Kyu Kim, Hong Luo, and J-Q Xi, Rep. Prog. Phys. **69**, 3069 (2006).

[2] J. R. Lakowicz, *Principles of Fluorescence Spectroscopy*, third ed. Springer, New York, 2006.

[3] Y.-H. Kwon, S.K. Shee, G.H. Gainer, G.H. Park, S.J. Hwang, J.J. Song, Appl. Phys. Lett. **76**, 840 (2000).

[4] R.Y. Korotkov, M.A. Reshchikov, B.M. Wessels, Physica B **1**, 325 (2003).

[5] D.G. Thomas, J.J. Hopfield, W.M. Augustyniak, Phys. Rev. **140** A202 (1965).

[6] N.C. Greenham et al., Chem. Phys. Lett. **89,** 241 (1995).

[7] A. Dementjev, V. Gulbinas, L. Valkunas, N. Ostapenko, S. Suto, A. Watanabe, J. Phys. Chem. C **111**, 4717 (2007).

[8] M. Shimizu, S. Suto, T. Goto, A. Watanabe, M. Matsuda, Phys. Rev. B **63**, 073403 (2001).

[9] K. Ebihara, S. Matsushita, S. Koshihara, F. Minami, T. Miyazawa, K. Obata, M. Kira, J. Lumin. **43,** 72 (1997).

[10] S. Zhou, Z. Fu, J. Zhang, S. Zhang, J. Lumin. **118**, 1979 (2006).

[11] E. Zych, C. Brecher, A.J. Wojtowicz, H. Lingertat, J. Lumin. **75**, 193 (1997).

[12] *Phosphor Handbook*, Sh. Shionoya W. M. Yen (Eds.), CRC Press, Boca Raton, 1999.

[13] M. R. Krames, M. Ochiai-Holcomb, G. E. Höfler, C. Carter-Coman, E. I. Chen, I.-H. Tan, P. Grillot, N. F. Gardner, H. C. Chui, J.-W. Huang, S. A. Stockman, F. A. Kish, M. G. Craford, T. S. Tan, C. P. Kocot, M. Hueschen, J. Posselt, B. Loh, G. Sasser, and D. Collins, Appl. Phys. Lett. **75**, 2365 (1999).

[14] J. J. Wierer, D. A. Steigerwald, M. R. Krames, J. J. O'Shea, M. J. Ludowise, G. Christenson, Y.-C. Shen, C. Lowery, P. S. Martin, S. Subramanya, W. Götz, N. F. Gardner, R. S. Kern, and S. A. Stockman, Appl. Phys. Lett. **78**, 3379 (2001).

LIST OF PUBLICATIONS RELATED TO THE THESIS

Papers

P1.   G. Tamulaitis, J. Mickevičius, **P. Vitta**, A. Žukauskas, M. S. Shur, Q.Fareed, and R. Gaska, "Time- and frequency-domain measurements of carrier lifetimes in GaN epilayers," Superlatt. Microstruct. **40**, 274-278 (2006).

P2.   G. Tamulaitis, J. Mickevičius, **P. Vitta**, M. S. Shur, K. Liu, Q. Fareed, J. P. Zhang, and R. Gaska "Carrier lifetimes in GaN revealed by stydying photoluminescence decay in time and frequency domains," ECS Transactions **3**, 307-314 (2006).

P3.   A. Katelnikovas, **P. Vitta**, P. Pobedinskas, G. Tamulaitis,A. Žukauskas, J. E. Jørgensen, and A. Kareiva. "Photoluminescence in sol gel-derived YAG:Ce phosphors," J. Cryst. Growth **304**, 361-368 (2007).

P4.   **P. Vitta**, P. Pobedinskas, and A. Žukauskas "Phosphor thermometry in white light-emitting diodes," IEEE Photonic Technol. Lett. **19**, 399-401 (2007).

P5.   J. Mickevičius, G. Tamulaitis, **P. Vitta**, A. Žukauskas, M.S. Shur, J. Zhang, J. Yang, and R. Gaska "Carrier dynamics in GaN at extremely low excited carrier densities," Solid State Commun. **145,** 312-315 (2008).

P6.   J. Mickevičius, **P. Vitta**, G. Tamulaitis, A. Žukauskas, M.S. Shur, J. Zhang, J. Yang, and R. Gaska "Luminescence decay kinetics in GaN studied by frequency domain measurements," Acta Phys. Pol. A **113**, 833-837 (2008).

P7.   K. Kazlauskas, A. Dementjev, V. Gulbinas, L. Valkunas, **P. Vitta**, A. Žukauskas, N. Ostapenko, and S. Suto "Temperature independent exciton relaxation in poly(di-n-hexylsilane) confined in nanoporous silica," Chem. Phys. Lett. **456**, 261-264 (2008).

P8.   D. Tomkutė-Lukšienė, T. Malinauskas, A. Stanišauskaitė, V. Getautis, K. Kazlauskas, **P. Vitta**, A. Žukauskas, and S. Juršėnas, "Efficient phosphorescent bis-cyclometallated iridium complex based on triazole-quinoline ligand," J. Photochem. Photobiol. A **198**, 106-110 (2008).

P9.   **P. Vitta** and A. Žukauskas "Thermal characterization of light-emitting diodes in the frequency domain," Appl. Phys. Lett. **93**, 103508 (2008).

P10. **P. Vitta** and A. Žukauskas, "Thermal characterization of light-emitting diodes in the frequency domain," Phys. Status Solidi C **6**, S887-S880 (2009).

P11. A. Katelnikovas, T. Bareika, **P. Vitta**, T. Jüstel, H. Winkler, A. Kareiva, A. Žukauskas, and G. Tamulaitis "YMgAlSiO:Ce phosphors - prospective for warm-white light emitting diodes," Opt. Mater. **32**, 1261 (2010).

P12. **P. Vitta**, I. Reklaitis, and A. Žukauskas „Phase resolved fluorescence lifetime measurements in the presence of high background signals," Sens. Act. B (submitted).

Conference contributions

K1.   **P. Vitta**, A. Žukauskas, A. Novičkovas, M. S. Shur, R. Gaska, "Puslaidininkiniu šviestuku sužadintos fotoliuminescencijos gesimo trukmės matavimai dažninės skyros metodu", 36-ji Lietuvos nacionalinė fizikos konferencija. Programa ir pranešimų tezės (Vilnius, 2005 m. birželio 16–18 d.), p. 68.

K2. A. Zukauskas, J. Mickevicius, **P. Vitta**, G. Tamulaitis, M. Shur, R. S. Qhalid Fareed, J. P. Zhang, and R. Gaska, "Carrier dynamics in GaN epilayers revealed by time- and frequency-domain measurements," Int. Conf. Blue Lasers and Light Emitting Diodes ISBLLED 2006. Programme and Abstract Book (Montpellier, France, May 15–19, 2006), p. 72–73.

K3. **P. Vitta**, P. Pobedinskas, and A. Zukauskas, "Phosphor thermometry in a white LED," Int. Conf. Blue Lasers and Light Emitting Diodes ISBLLED 2006. Programme and Abstract Book (Montpellier, France, May 15–19, 2006), p. 106-107.

K4. K. Kazlauskas, S. Jursenas, **P. Vitta**, A. Zukauskas, V. Getautis, and J. Grazulevicius, „Application of UV LED based frequency-domain fluorometry for estimation of fluorescence lifetime in organic LED compounds," Programme and Abstract Book (Montpellier, France, May 15–19, 2006), p. 117-118.

K5. A. Michalevičiūtė, J. Simokaitienė, J. V. Gražulevičius, K. Kazlauskas, **P. Vitta**, A. Žukauskas, and S. Juršėnas, "Optical properties of blue light-emitting carbazole derivatives for organic light-emitting diodes," 10th Eur. Conf. Organised Films. Book of Abstracts (Riga, Latvia, August 20–24, 2006), p. 96.

K6. G. Tamulaitis, J. Mickevicius, **P. Vitta**, A. Zukauskas, M. S. Shur, Q. Fareed, J. P. Zhang, and R. Gaska, "Study of yellow luminescence in GaN using photoluminescence spectroscopy in time and frequency domains," Eur. Workshop on III-Nitride Semiconductor Materials and Devices (EW3NS). Programme (Heraklion, Crete, Greece, September 18–20, 2006), p. 85.

K7. G. Tamulaitis, J. Mickevičius, **P. Vitta**, A. Žukauskas, M. S. Shur, K. Liu, Q. Fareed, J. P. Zhang, and R. Gaska, "Carrier lifetimes in GaN revealed by studying photoluminescence decay in time and frequency domains," 210th Meeting of the Electrochemical Society. Meeting Abstracts (Cancun, Mexico, October 29 – November 3, 2006).

K8. J. Mickevičius, **P. Vitta**, G. Tamulaitis, A. Žukauskas, M.S. Shur, J. Zhang, J. Yang, and R. Gaska, „Luminescence decay kinetics in GaN studied by frequency-domain measurements,"13th Int. Symp. Ultrafast Phenomena in Semiconductors, Abstract (Vilnius, August 26-29, 2007) p. 79.

K9. **P. Vitta**, T. Bareika, G.Tamulaitis, A. Žukauskas, A. Katelnikovas, A. Kareiva, „Photoluminescence analysis of sol-gel derived YAG:Ce phosphors," 9-th Int. Conf. - School „Advanced materials and technologies". Abstract (Palanga, 2007 rugpjūčio 27–31).

K10. T. Malinauskas, V. Getautis, D. Tomkutė-Lukšienė, K. Kazlauskas, **P. Vitta**, A. Žukauskas, S. Juršėnas, V. Gaidelis, and V. Jankauskas, "Phosphorescent iridium (III) complexes possessing charge transporting fragments," 7th Int. Conf. Electroluminescence of Molecular Materials and Related Phenomena, ICEL-7. Program and Abstracts (Dresden, Germany, September 2–6, 2008), p. 161.

K11. **P. Vitta** and A.Žukauskas „Thermal Characterization of Light-Emitting Diodes in the Frequency Domain," Abstracts of the International Workshop on Nitride semiconductors IWN2008 (Montreux, Switzerland October 6–10, 2008), p. 513.

K12. **P. Vitta**, Z. Vaitonis, A. Žukauskas, „Puslaidininkinių šviestukų šiluminis charakterizavimas," 38-ji Lietuvos nacionalinė fizikos konferencija, programa ir pranešimų tezės (Vilnius, 2009 m. birželio 8–10 d.), p. 264.

K13. **P. Vitta**, I. Reklaitis, and A. Žukauskas, "Fluorescence lifetime measurements in the frequency domain in the presence of high in-phase background," 38-ji Lietuvos nacionalinė fizikos konferencija, programa ir pranešimų tezės (Vilnius, 2009 m. birželio 8–10 d.), p. 44.

K14. **P. Vitta**, I. Reklaitis, and A. Žukauskas, "Fluorescence lifetime measurements in the frequency domain in the presence of high in-phase background," 11th Int. School-Conf. Advanced Materials and Technologies. Abstracts (Palanga, August 27–31, 2009), p. 44.

K15. **P. Vitta**, Z. Vaitonis, and A. Žukauskas, „Thermal Characterization of Light-Emitting Diodes" XXXVIII International School and Conference on the Physics of Semiconductors „Jaszowiec" 2009 Abstracts (Krynica-Zdroj, Poland June 19–26, 2009), p. 63.

LIST OF PAPERS AND PATENTS (APPLICATIONS) NOT INCLUDED TO THE THESIS:

P13. A. Žukauskas, A. Novičkovas, **P. Vitta**, M. S. Shur, and R. Gaska, "Raman measurements in water using a high-power light-emitting diode," J. Raman Spectrosc. **34**, 471-473 (2003).

P14. A. Žukauskas, K. Breivė, Z. Bliznikas, A. Novičkovas, **P. Vitta**, R. Vaicekauskas, A. Navickas, R. Gaska, and M. S. Shur, "Puslaidininkinė lempa šviesos terapijai," Elektronika ir elektrotechnika **5,** 38-42 (2003).

P15. **P. Vitta**, A. Žukauskas, R. Gaska, and M. S. Shur, "White complementary solid-state lamp," Leukos **1,** 59-66 (2004).

P16. A. Zukauskas, R. Vaicekauskas, F. Ivanauskas, G. Kurilcik, Z. Bliznikas, K. Breive, J. Krupic, A. Rupsys, A. Novickovas, **P. Vitta**, A. Navickas, V. Raskauskas, M. S. Shur, and R. Gaska, "Quadrichromatic white solid-state lamp with digital feedback," Proc. SPIE **5187**, 185-198 (2004).

P17. A .Žukauskas, **P. Vitta**, A. Novickovas, N. Kurilcik, S. Jursenas, H. Calkauskas, and R. Gaska, "AlGaN-based deep-UV LEDs for fluorescence sensing," Proc. SPIE **5617**, 249-260 (2004).

P18. **P. Vitta**, N. Kurilčik, S. Juršėnas, A. Žukauskas, E. Bakienė, J. Zhang, T. Katona, Y. Bilenko, A. Lunev, X. Hu, J. Deng, and R. Gaska, "Fluorescence-lifetime identification of biological agents using deep ultraviolet light-emitting diodes," Proc. SPIE **5990**, 233-246 (2005).

P19. **P. Vitta**, N. Kurilčik, S. Juršėnas, A. Žukauskas, A. Lunev, Y. Bilenko, J. Zhang, X. Hu, J. Deng, T. Katona, and R. Gaska, "Deep-UV light-emitting diodes for frequency-domain measurements of fluorescence lifetime in basic biofluorophores," Appl. Phys. Lett. **87**, 084106, 3 p. (2005).

P20. N. Kurilčuk, **P. Vitta**, A. Žukauskas, R. Gaska, A. Ramanavičius, A. Kaušaitė, and S. Juršėnas. "Fluorescence detection of biological objects with ultraviolet and visible light-emitting diodes," Optica Applicata **36**, 193-198 (2006).

P21. A. Žukauskas, N. Kurilčik, **P. Vitta**, S. Juršėnas, E. Bakienė, and R. Gaska "Optimization of a UV light-emitting diode based fluorescence-phase sensor," Proc. SPIE **6398**, Y1–Y14 (2006).

P22. **P. Vitta**, A. Žukauskas, R. Gaska, and M. Shur, "White light-emitting device and method," US Patent No 7,095,056 (2006).

P23. A. Urbonavičiūtė, P. Pinho, G. Samuolienė, P. Duchovskis, **P. Vitta**, A. Stonkus, G. Tamulaitis, A. Žukauskas, and L. Halonen "Effect of short-wavelength light on lettuce growth and nutritional quality," Sodininkystė ir daržininkystė **26**, 157-165 (2007).

P24. A. Urbonavičiūtė, P. Pinho, G. Samuolienė, P. Duchovskis, **P. Vitta**, A. Stonkus, G. Tamulaitis, A. Žukauskas, and L. Halonen, „Influence of bicomponent complimentary illumination on development of radish," Sodininkystė ir daržininkystė **26**, 309-316 (2007).

P25. A. Žukauskas, **P. Vitta**, N. Kurilčik, S. Juršėnas and E. Bakienė "Biological applications of frequency-domain fluorescence lifetime measurements using ultraviolet light-emitting diodes," Opt. Mater. **30**, 800-805 (2008).

P26. Z. Vaitonis, **P. Vitta**, and A. Žukauskas, "Measurement of the junction temperature in high-power light-emitting diodes from the high-energy wing of the electroluminescence band," J. Appl. Phys. **103**, 093110 (2008).

P27. A. Žukauskas, P. Duchovskis, Z. Bliznikas, G. Samuolienė, A. Urbonavičiūtė, **P. Vitta** „Žalingų nitratų kiekio augaluose sumažinimo, apšvitinant kietakūnio šviestuvo sukuriamu šviesos srautu, būdas ir įrenginys," Lietuvos respublikos patentas, Nr. 5516, (2008 09 25).

P28. A. Žukauskas, P. Duchovskis, Z. Bliznikas, G. Samuolienė, A. Urbonavičiūtė, and **P. Vitta**, "Method and apparatus for the reduction of harmful nitrates in plants using radiant flux generated by a solid-state illuminator," PCT Patent App. No. WO2008048080 (2008).

P29. **P. Vitta**, G. Tamulaitis, D. Shevchenko, A. Žukauskas, N. Starzhinskiy, K. Katrunov, and V. Ryzhikov, "Luminescence study of ZnSe based scintillators in frequency domain," Lith. J. Phys **48**, 243-247 (2008).

P30. A. Žukauskas, R. Vaicekauskas, F. Ivanauskas, H. Vaitkevičius, **P. Vitta**, and M. S. Shur "Statistical approach to color quality of solid-state lamps," IEEE Sel. J. Sel Top. Quantum Electron. **15**, 1189-1198 (2009).

P31. M. Karaliūnas, **P. Vitta**, A. Žukauskas, A. Zahnd, D. Bista, B. B. Chhetri, and M. R. Updhyaya "Characterization of Nepali Solid-state Lamps" Elektronika ir Elektrotechnika **1** (89), 29-34 (2009).

P32. Z. Bliznikas, K. Breivė, A. Novičkovas, **P. Vitta**, and A. Žukauskas, "Solid-State lamp for the improvement of nutritional quality of leafy vegetables," Elektronika ir Elektrotechnika **8** (96), 47-50 (2009).

P33. J. Mickevičius, G. Tamulaitis, **P. Vitta**, A. Žukauskas, N. Starzhinskiy, and V. Ryzhikov, "Characterization of ZnSe(Te) scintillators by frequency domain luminescence lifetime measurements," Nucl. Instr. and Meth. A **610**, 321-324 (2009).

P34. G. Samuolienė, A. Urbonavičiūtė, P. Duchovskis, Z. Bliznikas, **P. Vitta**, and A. Žukauskas, "Decrease in nitrate concentration in leafy vegetables under solid-state illuminator," HortScience **44**, 1857-1860 (2009).

P35. A. Urbonavičiūtė, G. Samuolienė, S. Sakalauskienė, A. Brazaitytė, J. Jankauskienė, P. Duchovskis, V. Ruzgas, A. Stonkus, **P. Vitta**, A. Žukauskas, and G. Tamulaitis, "Effect of flashing amber light on nutritional quality of green sprouts," Agronomy Res. **7**, 761-767 (2009).

P36. A. Žukauskas, R. Vaicekauskas, F. Ivanauskas, H. Vaitkevičius, **P. Vitta**, and M. Shur "New statistical figures of merit for color quality of solid-state lamps" ECS Transactions **19,** 13-20 (2009).

P37. A. Žukauskas, R. Vaicekauskas, F. Ivanauskas, H. Vaitkevičius, **P. Vitta**, and M. S. Shur, "Multiwavelength solid-state lamps with an enhanced number of rendered colors,"PCT Patent App. No WO2009102745 (2009).

P38. A. Žukauskas, R. Vaicekauskas, F. Ivanauskas, H. Vaitkevičius, **P. Vitta**, and M. S. Shur, "Solid-state lamps with complete conversion in phosphors for rendering and enhanced number of colors,"PCT Patent App. No WO2009117286 (2009).

P39. A. Žukauskas, R. Vaicekauskas, F. Ivanauskas, H. Vaitkevičius, **P. Vitta**, and M. S. Shur, "Solid-state lamps with partial conversion in phosphors for rendering and enhanced number of colors,"PCT Patent App. No WO2009117287 (2009).

P40. N. Ryškevič, S. Juršėnas, **P. Vitta**, E. Bakienė, R. Gaska, and A. Žukauskas "UV light-emitting diode based fluorescence sensor conceptional design for real-time bioparticle detection," Sens. Actuat. B, doi:10.1016/j.snb.2010.05.042 (accepted, 2010).

Information about the author

Name and Surname: **Pranciškus Vitta**

Natal day and place: 1982, 25th of November, Vilnius, Lithuania

Residence: Krakiškių sodų 12-oji st. 13, Vilnius, LT-14288, Lithuania

e-mail: pranciskus.vitta@ff.vu.lt

Education:

2000	Vilnius „Gerosios Vilties" secondary school
2004	Bachelor degree in Physics, Vilnius University
2006	Master degree in Physics, Vilnius University
2006-2010	Doctoral studies at Vilnius University

Scientific experience:

2002-2008	Engineer at the Institute of Applied Research, Vilnius University (part-time)
2008-till now	Junior scientific researcher at the Institute of Applied Research, Vilnius University (part-time)

Specialization: Application of light-emitting diodes in measurements and solid-state lighting solutions. Optical and electrical characterization of LEDs.

Publications: Co-author of 32 articles (22 in journals listed in WOS ISI) and 37 conference contributions, 2 patents (1 US PTO, 1 LT) and 4 PCT patent applications.